Cytosolic Delivery of Functional Proteins *In Vitro* through Tunable Gigahertz Acoustics

Shuting Pan[1,†,‡], Taewon Jeon[1,†,§], David C. Luther[†], Xuexin Duan[,‡], Vincent M. Rotello*[,†]*

† Department of Chemistry, University of Massachusetts, 710 North Pleasant Street, Amherst, Massachusetts 01003, United States

‡ State Key Laboratory of Precision Measuring Technology & Instruments, College of Precision Instrument and Optoelectronics Engineering, Tianjin University, Tianjin 300072, China.

§ Molecular and Cellular Biology Graduate Program, University of Massachusetts Amherst, 710 N. Pleasant St., Amherst, United States

KEYWORDS: GHz acoustics, hydrodynamics, protein delivery, cytosolic delivery

ABSTRACT: Intracellular delivery is essential to therapeutic applications such as genome engineering and disease diagnosis. Current methods lack simple, non-invasive strategies, and are often hindered by long incubation time or high toxicity. Hydrodynamic approaches offer rapid and controllable delivery of small molecules, but thus far have not been demonstrated for delivering functional proteins. In this work, we developed a robust hydrodynamic approach based on gigahertz (GHz) acoustics to achieve rapid and non-invasive cytosolic delivery of biologically active proteins. With this method, GHz-based acoustic devices trigger oscillations through a liquid medium (acoustic streaming) generating shear stress on the cell membrane and

inducing transient nanoporation. This mechanical effect enhances membrane permeability and enables cytosolic access to cationic proteins without disturbing their bioactivity. We evaluated the versatility of this approach through delivery of cationic fluorescent proteins to a range of cell lines, all of which displayed equally efficient delivery speed (≤ 20 minutes). Delivery of multiple enzymatically active proteins with functionality related to apoptosis or genetic recombination further demonstrated the relevance of this method.

1. INTRODUCTION

On-demand drug, nanomaterial and biomolecule delivery into cells has emerged as a promising research field for numerous biomedical applications.[1,2] Proteins in particular provide a transient method for modifying and diagnosing cell states *in vitro* and *ex vivo*.[3,4] Current methods for introduction of therapeutic or imaging species into cells can be broadly separated into 'chemical' and 'physical' approaches. Chemical methods, such as nanoscale delivery vehicles[5-8] or covalent modification[9] have been studied extensively in recent years with great promise for translatability.[10] However, chemical delivery systems often require complex synthetic processes, are limited by cargo and cell type, and can face issues related to stability of both carrier and cargo.[11,12] Physical methods, such as microinjection,[13] thermal poration,[14] optoporation,[15] electroporation,[16,17] and acoustic sonoporation[18] have paved the way for intracellular delivery.[19] With these approaches, transient nanopores are generated in the plasma membrane that facilitate the rapid diffusion of exogenous molecules into cells before the pore is repaired. These methods notably avoid challenges associated with endosomal entrapment of delivery cargo. However, they have been known to cause irreversible damage to cells due to excessive physical disruption,

or reduced delivery efficiency due to inadequate stress, making physical parameters for delivery a key factor.

Recently, hydrodynamic-induced mechanical membrane deformation has emerged as an efficient tool for delivery of biomolecules[20, 21] and drug molecules[22-24] into cells. These methods are simple, controllable, and suitable for delivery of most macromolecules into a wide variety of cell types. Recently, we developed a novel hydrodynamic approach for transient cellular poration based on high frequency acoustic stimulation.[22] Controlled high speed acoustic streaming flow speeds (> m/s) were generated using our gigahertz-frequency (GHz) acoustic resonator,[25, 26] inducing shear stress that triggered gentle deformation of cell membranes and temporarily improved cell permeability.[22] Compared to other physical methods, acoustic streaming features a simple setup, robust instrumentation, and is generally less invasive. Our previous research has demonstrated GHz acoustic streaming could enhance cellular uptake of drug molecules[22] and nanomaterials, [27] however, intracellular delivery of biologically active species such as recombinant proteins has not yet been accomplished. In this work, schematically depicted in **Figure 1a,** we engineered a biologics delivery system by combining our hydrodynamic GHz acoustics approach with different biologically active proteins. Protein stability, delivery efficiency, and enzymatic activity after intracellular delivery under acoustic streaming conditions were evaluated in multiple cell lines. Overall this method provides a simple, efficient, and highly tunable platform for intracellular protein delivery.

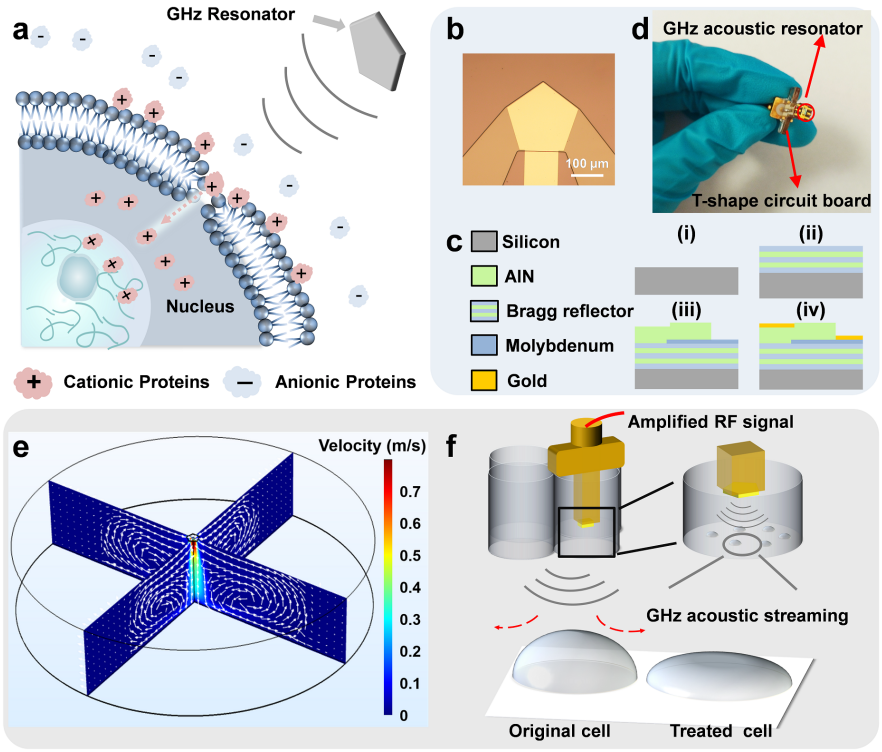

Figure 1. (a) General schematic of GHz acoustic-assisted cytosolic delivery of cationic proteins through transient poration. (b) Top view micrograph of the GHz resonator. (c) The fabrication process used to generate the device. (d) Photograph of the GHz resonator sealed on a T-shaped circuit board and applied in a 96-well plate. (e) 3D FEM analysis of GHz acoustic streaming. (f) Scheme of the working mechanism of GHz acoustics system.

2. RESULTS AND DISCUSSION

Cytosolic delivery of fluorescent proteins using GHz acoustics

We used an acoustic hydrodynamic approach to facilitate direct protein delivery into the cell cytosol. As schematically shown in **Figure 1a**, upon treatment with GHz acoustic streaming, cationic proteins are spontaneously delivered through transient membrane poration. A top-view

micrograph of the GHz acoustic resonator is shown in **Figure 1b**, and the fabrication process **(Figure 1c)** is described in Methods. The GHz acoustic device is designed to be inserted into a standard 96-well plate, as shown in **Figure 1d**. The GHz acoustic resonator triggers strong acoustics-based currents through a liquid medium due to the ultra-high resonator frequency (1.65 GHz).[25] The mechanism of flow motion has been characterized by 3D simulation, as shown in **Figure 1e**. The generated acoustic streaming can induce shear stress to the cell membrane, which causes mechanical deformation (**Figure 1f and Figure S2)**, and eventually generates transient nanopores that are permeable to sub-micron sized species, as reported in our previous work.[22] Green fluorescent protein (GFP, 37 kDa, -7 net charge) and supercharged GFP (+25GFP, 37 kDa, +25 net charge) were expressed as described in Methods. GFP was chosen as a model protein for its robust fluorescence (488/509 nm) and ability to translocate to the nucleus, allowing for rapid detection of cytosolic delivery.[28] After acoustic treatment, confocal microscopy was employed to visualize protein stability and delivery efficiency. We observed that +25GFP was efficiently delivered to the cytosol (**Figure 2a**), while control samples with no acoustic treatment **(Figure 2b)** showed no uptake. Significantly, the analogous anionic wild-type GFP was not delivered under the same acoustic treatment conditions (**Figure S4**). As shown in **Figure 2a**, +25GFP remains fluorescent after delivery, demonstrating the retention of protein structure through acoustic treatment. This result suggested that cationic surface charge was necessary to provide initial electrostatic interaction between the protein and the anionic cell membrane.

After cytosolic delivery, +25GFP is able to pass through the nuclear pore by passive diffusion due to its small size relative to the diameter of the nuclear pore (~40 kDa).[28,29] Nuclear co-localization of fluorescence signal is thus an effective approach to determining cytosolic delivery of small fluorescent proteins like GFP. Cells treated with GHz acoustic streaming displayed

overlapping fluorescence between +25GFP (FITC) and Hoechst nuclear stain (DAPI), consistent with nuclear localization **(Figure 2a)**. This result is consistent with direct cytosolic delivery of +25GFP by GHz acoustic streaming. Confocal microscopy Z-stacking was conducted to further illustrate cytosolic localization of delivered protein (supplementary movie 1). Alamar Blue cytotoxicity evaluation revealed negligible toxicity after treatment (**Figure 2c)**.

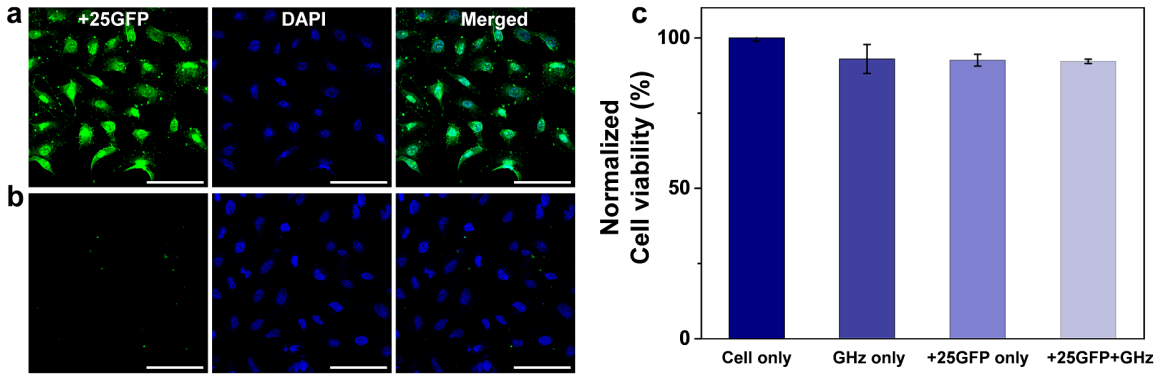

Figure 2. Representative confocal images showing cytosolic delivery of +25GFP. (a) HeLa cells treated with +25GFP and 400 megawatts (mW) GHz acoustics treatment for 20mins. Scale bars: 100 μm (b) HeLa cells incubated +25GFP without GHz acoustics for 20mins. Scale bars: 100 μm (c) Alamar Blue cell viability assay. Four groups included, cells without +25GFP and GHz acoustics treatment (Cell only), cells with only GHz acoustics treatment (GHz only), cells with only +25GFP treatment (+25GFP only) and cells with both +25GFP and GHz acoustics treatment (+25GFP+GHz).

Optimal working conditions for delivery were determined by parametrically varying amplitude (power) using the GHz resonator. As shown in **Figure 3**, cell viability was not greatly influenced increasing power from 200mW to 400mW, while increasing beyond this point to 500mW decreased viability by ~42%. Partial cell detachment from poly-L-lysine (PLL)-treated plates was observed when higher acoustic power was applied (≥500 mW). Cell viability was overlaid with mean fluorescence intensity (MFI) to correlate resonator power with delivery efficiency. With increasing applied power from 200 to 400mW, the intracellular level of +25GFP increases, suggesting that delivered dose of protein is power-dependent. As described previously,[25, 30]

streaming speed is linearly proportional to resonator power. Higher speed streaming generates larger hydrodynamic forces, enhancing cellular uptake. Faster streaming also likely increases protein-membrane interactions due to increased fluid flow. Based on these experimental observations, 400mW was considered as the optimized amplitude of applied power, and was used for subsequent studies.

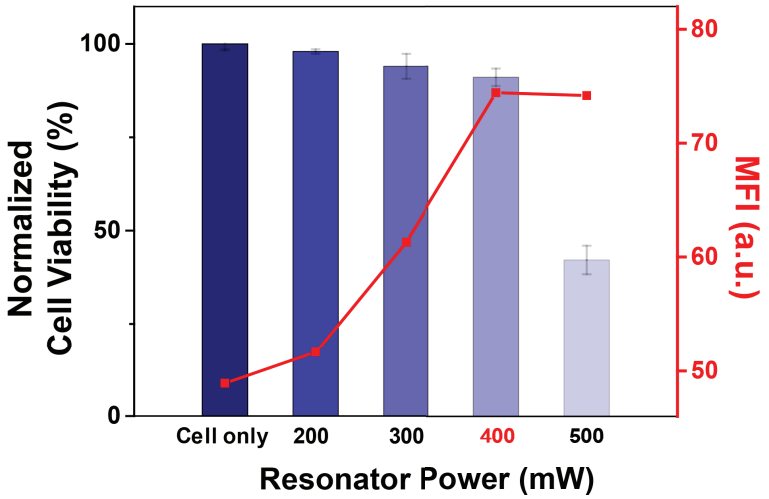

Figure 3. Viability and delivery efficiency-based power optimization for intracellular protein delivery. Cell viability and mean fluorescence intensity (MFI) were investigated in HeLa cells after acoustic treatment at varied power (200mW, 300mW, 400mW and 500mW) for 20 min.

GHz-mediated delivery of active functional proteins

The delivery of two cationic enzymes, (granzyme A (GzmA) and cytochrome C (CytC)) was next investigated. Cell viability *via* Alamar Blue was used as a metric to evaluate intracellular delivery of functional protein.[31,32] As demonstrated in **Figure 4a**, after GHz acoustic streaming alone and 24 h incubation, no decrease in cell viability was observed. However, after GHz acoustic-enhanced GzmA delivery and 24 h incubation, cell viability was dramatically decreased

(≤8%), while there was no obvious reduction for cells treated with GzmA alone (no acoustic treatment). A similar result was observed for CytC delivery, with cell viability decreasing to ≤25%, while control groups without acoustic treatment remained fully viable. We further sought to investigate if this effect was indeed caused by apoptosis through staining with YO-PRO-1, a fluorescent dye that selectively permeates apoptotic cells. As shown in **Figure 4b**, after acoustics-mediated delivery of GzmA, visible fluorescence suggests not only successful delivery of protein, but retention of pro-apoptotic activity.

We further sought to investigate if this system could be applicable for the delivery of an enzymatically active nuclease enzyme. Cre recombinase is a cationic nuclease that performs a targeted genetic recombination at 'LoxP' recognition sites in DNA.[33, 34] For these studies we utilized our previously described HEK-293T reporter cell line.[35] If successful recombination occurs, there will be a fluorescence switch from dsRed (588/583 nm) to GFP. As shown in **Figure 4c**, after 20 mins delivery and 48 h incubation to allow for total genetic recombination, HEK reporter cells that underwent GHz acoustics-enhanced Cre delivery converted from red (TRITC) to green (FITC) fluorescence, while control group cells (no acoustics treatment) retained their dsRed expression (**Figure 4d**). This study demonstrates the capability of our GHz acoustics delivery approach to introduce an active nuclease into the cell, but further represents the ability of this approach to deliver proteins directly to the cytosol, providing access to the nucleus.

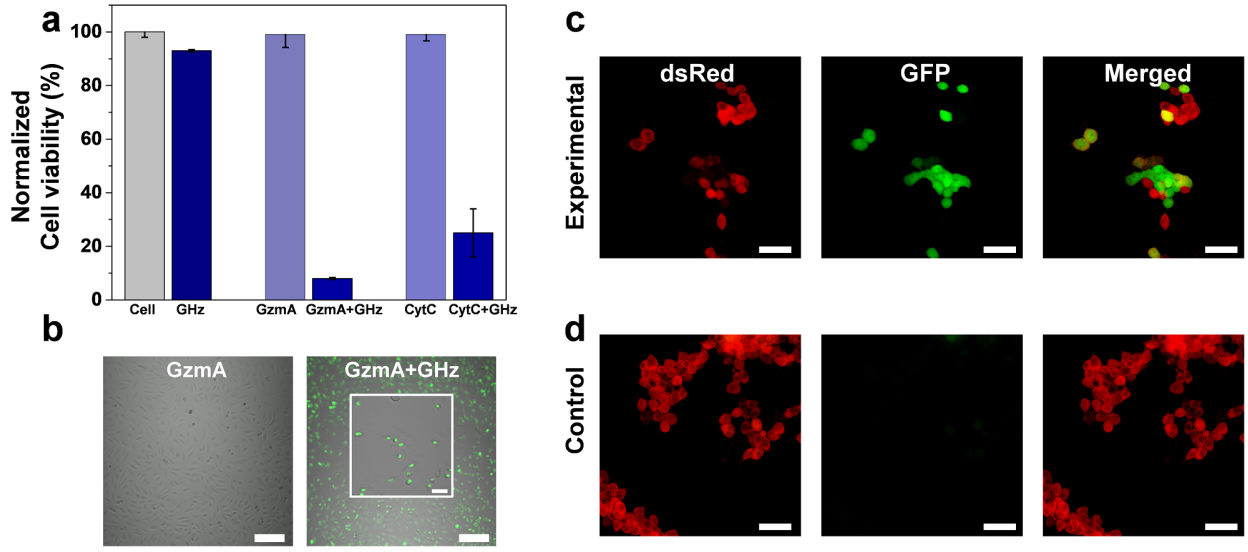

Figure 4. Functional delivery of GzmA, CytC, and Cre recombinase. (a) Cell viability evaluation for delivery of GzmA and CytC with and without GHz acoustics treatment at 400mW for 20mins. (b) Confocal YO-PRO-1 staining. Scale bars: 200 μm. Enlarged image shows accumulation of protein in nucleus. Scale bar: 50 μm. GHz acoustic-assisted Cre delivery provides genetic recombination (c) with no function in control group (d). Scale bars: 50 μm. GFP expression was switched on and green fluorescence was accordingly observed after successful delivery of Cre.

GHz-mediated delivery is versatile and ATP-independent

Generalizability of the GHz acoustics delivery platform is largely dependent on two factors: (1) energy dependence, and (2) cell type specificity. As a critical energy source for most active cellular internalization pathways, adenosine triphosphate (ATP) dependence provides fundamental information on uptake mechanism, specifically related to endocytosis.[36-38] Cells were pre-treated with a modified ATP-depletion media (details available in Methods) and then delivered under standard conditions. Cells treated with GHz acoustics experienced equally efficient delivery, regardless of ATP depletion **(Figure 5)**. This result is consistent with poration caused by the acoustic streaming being the primary mechanism of uptake, as opposed to an endocytic pathway. Notably, the poration process is transient, as indicated by the absence of

wild-type GFP uptake **(Figure S4)**, whereas prolonged pore lifetime would allow free diffusion into the cells, or decreased viability.

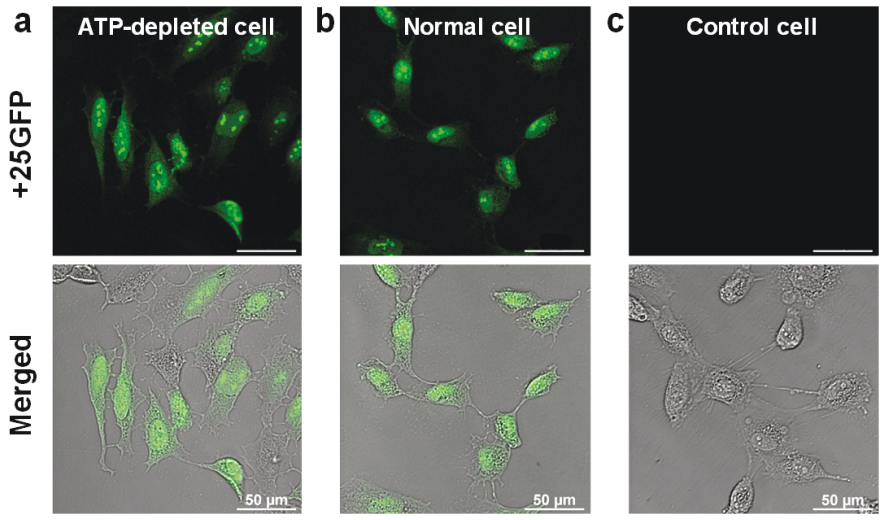

Figure 5. +25GFP delivery under ATP-depleted conditions. (a) Cells after 30 min ATP depletion show uptake of +25GFP. (b) Normally cultured cells under GHz acoustics-assisted protein delivery. (c) Cells treated with +25GFP alone show no obvious uptake. All scale bars: 50 μm

Generalizability of the acoustic delivery method was further investigated using different mammalian cell lines. In addition to HeLa cells (human cervical cancer), we utilized 3T3 (murine endothelial), RAW 264.7 (murine macrophage) and HEK-293T cells (human endothelial) to evaluate cell type dependence of the GHz acoustics-enhanced approach. Confocal images in **Figure 6** show +25GFP delivery into these three cell lines. Efficient cytosolic delivery of +25GFP was observed with acoustic treatment, while no +25GFP fluorescence could be detected in the control group (no acoustic treatment). These results collectively demonstrate the generalizability of this GHz acoustics strategy for cationic protein delivery.

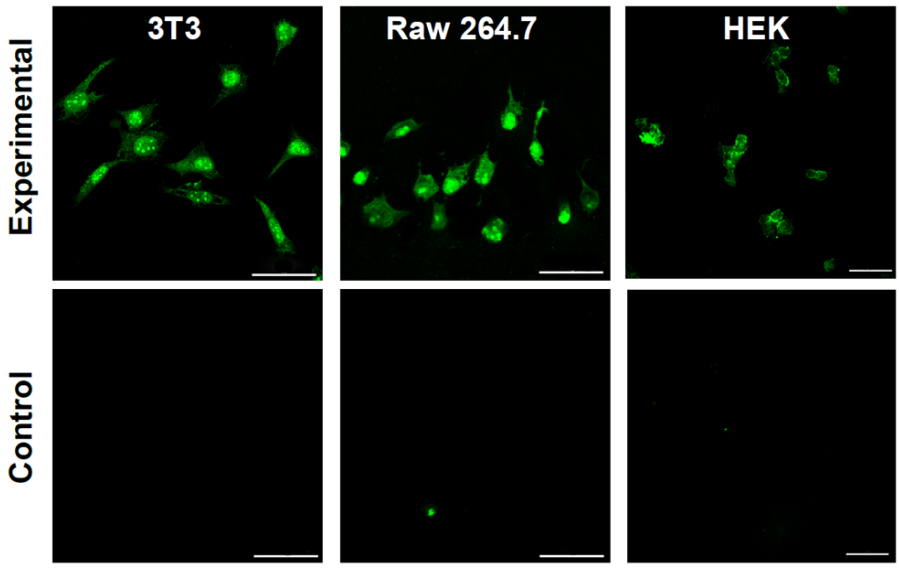

Figure 6. Confocal images showing +25GFP delivery with different cell lines. 3T3, RAW 264.7, and HEK- 293T cells were treated with 400mW GHz acoustics treatment in the presence of +25GFP for 20mins. Controls were incubated with same amount of +25GFP without GHz acoustics for 20mins. All scale bars: 50 μm

3. CONCLUSIONS

In summary, we present a GHz acoustics-based hydrodynamic approach for direct cytosolic delivery of cationic proteins. GHz acoustic streaming transiently improves permeability of the cell membrane and allows for cytosolic entry of cationic protein species. Using this approach, several cationic proteins were delivered into cells with high efficiency with no notable deleterious effects on the cells. This method retains the functionality of therapeutic proteins during the delivery process, suggesting that protein secondary structure is unaffected. Compared with conventional delivery strategies, the GHz acoustics approach provides an ATP-independent delivery pathway, avoiding issues associated with instability or multi-component delivery. This approach is highly effective in 2D cell culture, and in principle could also be applied to more complex targets such as skin or soft tissue. Overall, the simplicity and versatility of this method

suggests it would be highly suitable for applications in cell imaging and therapeutics, and could furthermore provide a powerful scaffold for hydrodynamic-based protein delivery platforms in the future.

4. EXPERIMENTAL SECTION

4.1. Proteins. Supercharged GFP (+25GFP, 37 kDa, pI: >11, net charge= +25)[39] was a gift from the David R. Liu Group.[40] Cre recombinase (38.5 kDa, pI: 9.4, net charge= +9), Granzyme A (29 kDa, pI= 8.69; net charge= +8), and Cytochrome C (12.4 kDa, pI= 9.37; net charge= +8) were expressed and purified according to our previous method.[41] Plasmids including Cre recombinase (Addgene id = 36915), Granzyme A (Addgene id = 8823), and Cytochrome C (Addgene id = 41182) were purchased from Addgene. For bacterial expression, genes were cloned into a bacterial expression vector (pET21b or pQE80) with 6xHis at the N-terminus. Recombinant proteins were expressed in E. coli BL21 Rosetta strain using a standard protein expression protocol. The purity of native proteins was determined using 8% and 12% SDS-PAGE gel, depending on protein size, and evaluated for aggregation via dynamic light scattering (DLS).

4.2. Cell Culture. 96-well plates were pre-treated with PLL (Sigma, USA) to prevent cellular detachment. 1×10^4 Cells were then seeded in a PLL-coated plate in the following media: low glucose DMEM (HeLa, RAW264.7 and 3T3); and high glucose DMEM (HEK-293T). All media contained 10% FBS and 1% penicillin/streptomycin antibiotics. Cells were grown overnight at 37 °C under 5% CO_2 and washed with 1X PBS prior to protein delivery. Cells were counted using a hemocytometer and standard cell culturing protocol.

4.3. Setup of Intracellular Delivery System. The GHz acoustic resonator with 1.65 GHz resonation frequency was fabricated using a complementary metal oxide semiconductor (CMOS) compatible technology; the fabrication process can be found in our previous work[25, 42] and is schematically shown in **Figure 1c**. Briefly, thin layers of silicon dioxide (SiO_2) and aluminium nitride (AlN) were alternately deposited on a silicon substrate using plasma enhanced chemical vapor deposition (PECVD) and RF reactive magnetron sputtering to form Bragg reflector layers (Figure 1c (ii)). A piezoelectric material sandwiched between two electrodes was utilized to trigger acoustics. Herein, a 600 nm molybdenum layer, serving as the bottom electrode was deposited by sputtering and then patterned by plasma etching, after which an AlN (1000 nm) layer was further deposited and patterned by reactive ion etching to form the piezoelectric layer, as shown in Figure 1c (iii). Finally, a 300 nm gold layer was evaporated and patterned by lift-off process to make up the top electrode and testing pads (Figure 1c (iv)). After fabrication, the GHz resonator was sealed on a T-shape circuit board, and the size of bottom end is 4 mm*4 mm, which is compatible with 96-well plate. RF signal generated by a signal generator (Agilent, N5181A) is amplified through a power amplifier (Mini-Circuits, ZHL-5W-422), and applied to the resonator. The power amplitude and mode of GHz acoustics was conveniently controlled and adjusted by the signal generator. The detail of this setup can be found in supporting information.

For protein delivery, 400 nM protein (e.g. supercharged GFP (+25GFP), Cytochrome C, Granzyme A or Cre) in 100 μL serum-free medium was applied to one well with adherent cells, and the device was inserted and fixed at the 1.5 mm relative distance between the its surface to cell. For experimental group, the resonator was triggered with amplified RF signal for 20 min followed by rinsing twice with PBS, while control group was only incubated for 20 min and same twice rinsing. For delivery, cells were removed from incubation to ambient temperature

briefly, and then returned to 37°C. After delivery, for delivery of multiple functional proteins, cells were incubated in DMEM media for another 24 h to allow protein activity.

4.4. Assessment of the protein delivery. Confocal microscopy (Zeiss LSM 510 Meta microscope or Nikon A1 laser scanning microscope) was utilized for evaluating the cellular uptake of proteins. After each delivery process, the cells were washed with PBS three times to remove free proteins. Then cells were then fixed with a 4% paraformaldehyde aqueous solution for 20 min at room temperature and rinsed with PBS. For co-localization of delivered payload, cells were stained with DAPI at room temperature for 10 min and rinsed with PBS. Afterwards, delivery efficiency was determined by confocal microscopy. Z-stacking was conducted using Nikon A1, at every 125 nm interval. The delivery efficiency was estimated by mean fluorescence intensity (MFI) of confocal images (as shown in **Figure S3**), which were further analyzed by NIS-Elements software and plotted in histogram form.

4.5. Cytotoxicity and Apoptosis assay. Alamar Blue assay was used to quantify the biocompatibility of the GHz acoustics assisted delivery system and the therapeutic efficiency of Cytochrome C (CytC) and Granzyme A (GzmA). Briefly, cells were seeded in a 96-well plate for 24 h prior to the experiment. On the day of experiment, the cells were treated with GHz acoustics, followed by washing with PBS and incubation in complete media supplemented with 10% Alamar blue assay reagent (Invitrogen, CA) for 3 h at 37ºC. Fluorescence intensity was then measured (excitation/emission: 560/ 590 nm) using a microplate reader. For investigating the therapeutic efficiency of delivered protein, cells were treated with CytC or GzmA in PBS for GHz acoustics treatment, and then incubated for an additional day, after which cells were washed with PBS and the cell viability was determined by Alamar blue assay. For apoptosis assay, the cells were treated with GzmA and one day incubation as above, afterwards the media was

replaced with fresh complete media containing 1mM YO-PRO-1 apoptotic staining reagent (ThermoFisher Scientific), and incubated for 30 min at 37 ^{o}C. Cells were washed with PBS for fluorescence imaging.

4.6. Cre/loxP Recombination System. To assess Cre recombinase activity, we used loxP-dsRed(STOP)-loxP-GFP HEK-293T cells that were generated through stable transfection as previously reported.[35] We delivered recombinant Cre recombinase with GHz acoustics treatment and the cells were allowed to grow for 48 h and then assessed by confocal microscopy for Cre activity by checking fluorescence changes.

4.7. Mechanism Study. ATP depletion was utilized to verify the mechanism of cell uptake of protein. Herein ATP-depletion solution (sodium azide, 10 mM; 2-deoxyglucose, 50 mM) was pretreated to cells at 37 °C for 1 h prior to delivery. Subsequently, the cells were treated with supercharged GFP as described.

ASSOCIATED CONTENT

Supporting Information. The Supporting Information is available free of charge on the ACS Publications website.

GHz acoustic streaming setup; GHz acoustic streaming and the induced cell membrane deformation; Confocal images for optimal working conditions; Investigation of cytosolic delivery of proteins with different surface charge (PDF)

Confocal microscopy Z-stacking for cytosolic localization of delivered +25GFP (AVI)

AUTHOR INFORMATION

Corresponding Author

*E-mail: rotello@chem.umass.edu

*E-mail: xduan@tju.edu.cn. Tel./Fax: +86 2227401002 (X.D.).

Author Contributions

SP, TJ, DCL, and VMR designed the experiments. SP operated the GHz acoustics instrument and directed the studies. TJ performed cell culture, expressed proteins, and performed confocal imaging. DCL assisted in experimental design and protein expression. XD and VMR supervised the project.

Notes

The authors declare no competing financial interest.

ACKNOWLEDGMENT

This research was supported by the NIH (EB022641), and the NSF (CHE-1808199). The authors would like to acknowledge Dr. James Chambers and the Light Microscopy Core Facility at UMass Amherst. X. Duan acknowledges support by the National Natural Science Foundation of China (NSFC No. 61674114, 91743110, 21861132001), National Key R&D Program of China (2017YFF0204604), Tianjin Applied Basic Research and Advanced Technology (17JCJQJC43600), and the 111 Project (B07014).

REFERENCES

1. Shen, B.; Ma, Y.; Yu, S.; Ji, C., Smart Multifunctional Magnetic Nanoparticle-based Drug Delivery System for Cancer Thermo-Chemotherapy and Intracellular Imaging. ACS Appl Mater Interfaces 2016, 8 (37), 24502-8.

2. Jiang, T.; Sun, W.; Zhu, Q.; Burns, N. A.; Khan, S. A.; Mo, R.; Gu, Z., Furin-Mediated Sequential Delivery of Anticancer Cytokine and Small-Molecule Drug Shuttled by Graphene. Adv Mater 2015, 27 (6), 1021-8.

3. Stewart, M. P.; Sharei, A.; Ding, X.; Sahay, G.; Langer, R.; Jensen, K. F., In Vitro and Ex Vivo Strategies for Intracellular Delivery. Nature 2016, 538 (7624), 183-192.

4. Mout, R.; Ray, M.; Yesilbag Tonga, G.; Lee, Y. W.; Tay, T.; Sasaki, K.; Rotello, V. M., Direct Cytosolic Delivery of CRISPR/Cas9-Ribonucleoprotein for Efficient Gene Editing. 2017, 11 (3), 2452-2458.

5. Shi, H.; Liu, S.; Cheng, J.; Yuan, S.; Yang, Y.; Fang, T.; Cao, K.; Wei, K.; Zhang, Q.; Liu, Y., Charge-Selective Delivery of Proteins Using Mesoporous Silica Nanoparticles Fused with Lipid Bilayers. ACS Appl Mater Interfaces 2019, 11 (4), 3645-3653.

6. Wang, M.; Zuris, J. A.; Meng, F.; Rees, H.; Sun, S.; Deng, P.; Han, Y.; Gao, X.; Pouli, D.; Wu, Q.; Georgakoudi, I.; Liu, D. R.; Xu, Q., Efficient Delivery of Genome-Editing

Proteins Using Bioreducible Lipid Nanoparticles. Proc Natl Acad Sci U S A 2016, 113 (11), 2868-73.

7. Sangsuwan, R.; Tachachartvanich, P.; Francis, M. B., Cytosolic Delivery of Proteins Using Amphiphilic Polymers with 2-Pyridinecarboxaldehyde Groups for Site-Selective Attachment. J Am Chem Soc 2019, 141 (6), 2376-2383.

8. Ma, Y.; Nolte, R. J.; Cornelissen, J. J., Virus-based Nanocarriers for Drug Delivery. Adv Drug Deliv Rev 2012, 64 (9), 811-25.

9. Jiang, Y.; Pan, X.; Chang, J.; Niu, W.; Hou, W.; Kuai, H.; Zhao, Z.; Liu, J.; Wang, M.; Tan, W., Supramolecularly Engineered Circular Bivalent Aptamer for Enhanced Functional Protein Delivery. J Am Chem Soc 2018, 140 (22), 6780-6784.

10. Yu, M.; Wu, J.; Shi, J.; Farokhzad, O. C., Nanotechnology for Protein Delivery: Overview and Perspectives. J Control Release 2016, 240, 24-37.

11. Gilleron, J.; Querbes, W.; Zeigerer, A.; Borodovsky, A.; Marsico, G.; Schubert, U.; Manygoats, K.; Seifert, S.; Andree, C.; Stoter, M.; Epstein-Barash, H.; Zhang, L.; Koteliansky, V.; Fitzgerald, K.; Fava, E.; Bickle, M.; Kalaidzidis, Y.; Akinc, A.; Maier, M.; Zerial, M., Image-based Analysis of Lipid Nanoparticle-mediated Sirna Delivery, Intracellular Trafficking and Endosomal Escape. Nat Biotechnol 2013, 31 (7), 638-46.

12. Lee, Y. W.; Luther, D. C.; Kretzmann, J. A.; Burden, A.; Jeon, T.; Zhai, S.; Rotello, V. M., Protein Delivery into the Cell Cytosol Using Non-Viral Nanocarriers. Theranostics 2019, 9 (11), 3280-3292.

13. Lappe-Siefke, C.; Maas, C.; Kneussel, M., Microinjection into Cultured Hippocampal Neurons: A Straightforward Approach for Controlled Cellular Delivery of Nucleic Acids, Peptides and Antibodies. J Neurosci Methods 2008, 175 (1), 88-95.

14. Sintov, A. C.; Krymberk, I.; Daniel, D.; Hannan, T.; Sohn, Z. e.; Levin, G., Radiofrequency-Driven Skin Microchanneling as A New Way for Electrically Assisted Transdermal Delivery of Hydrophilic Drugs. Journal of Controlled Release 2003, 89 (2), 311-320.

15 . Waleed, M.; Hwang, S. U.; Kim, J. D.; Shabbir, I.; Shin, S. M.; Lee, Y. G., Single-Cell Optoporation and Transfection Using Femtosecond Laser and Optical Tweezers. Biomed Opt Express 2013, 4 (9), 1533-47.

16. Choi, S. O.; Kim, Y. C.; Lee, J. W.; Park, J. H.; Prausnitz, M. R.; Allen, M. G., Intracellular Protein Delivery and Gene Transfection by Electroporation Using a Microneedle Electrode Array. Small 2012, 8 (7), 1081-91.

17. Cao, Y.; Ma, E.; Cestellos-Blanco, S.; Zhang, B.; Qiu, R.; Su, Y.; Doudna, J. A.; Yang, P., Nontoxic Nanopore Electroporation for Effective Intracellular Delivery of Biological Macromolecules. Proc Natl Acad Sci U S A 2019, 116 (16), 7899-7904.

18. Pitt, W. G.; Husseini, G. A.; Staples, B. J., Ultrasonic Drug Delivery–A General Review. Expert opinion on drug delivery 2004, 1 (1), 37-56.

19. Lakshmanan, S.; Gupta, G. K.; Avci, P.; Chandran, R.; Sadasivam, M.; Jorge, A. E.; Hamblin, M. R., Physical Energy for Drug Delivery; Poration, Concentration and Activation. Adv Drug Deliv Rev 2014, 71, 98-114.

20. Kizer, M. E.; Deng, Y.; Kang, G.; Mikael, P. E.; Wang, X.; Chung, A. J., Hydroporator: A Hydrodynamic Cell Membrane Perforator for High-Throughput Vector-Free Nanomaterial Intracellular Delivery and DNA Origami Biostability Evaluation. Lab Chip 2019, 19 (10), 1747-1754.

21. Deng, Y.; Kizer, M.; Rada, M.; Sage, J.; Wang, X.; Cheon, D. J.; Chung, A. J., Intracellular Delivery of Nanomaterials via an Inertial Microfluidic Cell Hydroporator. Nano Lett 2018, 18 (4), 2705-2710.

22. Zhang, Z.; Wang, Y.; Zhang, H.; Tang, Z.; Liu, W.; Lu, Y.; Wang, Z.; Yang, H.; Pang, W.; Zhang, H.; Zhang, D.; Duan, X., Hypersonic Poration: A New Versatile Cell Poration Method to Enhance Cellular Uptake Using a Piezoelectric Nano-Electromechanical Device. Small 2017, 13 (18).

23. Lu, Y.; de Vries, W. C.; Overeem, N. J.; Duan, X.; Zhang, H.; Zhang, H.; Pang, W.; Ravoo, B. J.; Huskens, J., Controlled and Tunable Loading and Release of Vesicles by Using Gigahertz Acoustics. Angew Chem Int Ed Engl 2019, 58 (1), 159-163.

24. Wang, F.; Wang, H.; Wang, J.; Wang, H. Y.; Rummel, P. L.; Garimella, S. V.; Lu, C., Microfluidic Delivery of Small Molecules into Mammalian Cells based on Hydrodynamic Focusing. Biotechnol Bioeng 2008, 100 (1), 150-8.

25 . Cui, W.; Pang, W.; Yang, Y.; Li, T.; Duan, X., Theoretical and Experimental Characterizations of Gigahertz Acoustic Streaming in Microscale Fluids. Nanotechnology and Precision Engineering 2019, 2 (1), 15-22.

26. Cui, W.; Zhang, H.; Zhang, H.; Yang, Y.; He, M.; Qu, H.; Pang, W.; Zhang, D.; Duan, X., Localized Ultrahigh Frequency Acoustic Fields Induced Micro-Vortices for Submilliseconds Microfluidic Mixing. Applied Physics Letters 2016, 109 (25).

27. Lu, Y.; Palanikumar, L.; Choi, E. S.; Huskens, J.; Ryu, J. H.; Wang, Y.; Pang, W.; Duan, X., Hypersound-Enhanced Intracellular Delivery of Drug-Loaded Mesoporous Silica Nanoparticles in a Non-Endosomal Pathway. ACS Appl Mater Interfaces 2019, 11 (22), 19734-19742.

28. Timney, B. L.; Raveh, B.; Mironska, R.; Trivedi, J. M.; Kim, S. J.; Russel, D.; Wente, S. R.; Sali, A.; Rout, M. P. Simple Rules for Passive Diffusion through the Nuclear Pore Complex. J. Cell Biol. 2016, 215 (1), 57–76.

29. Lusk, C.P.; King, M.C. The nucleus: keeping it together by keeping it apart. Curr. Op. in Cell Biol. 2017, 44. 44-50.

30. Pan, S.; Zhang, H.; Liu, W.; Wang, Y.; Pang, W.; Duan, X., Biofouling Removal and Protein Detection Using a Hypersonic Resonator. ACS Sens 2017, 2 (8), 1175-1183.

31. Martinvalet, D.; Dykxhoorn, D. M.; Ferrini, R.; Lieberman, J., Granzyme A Cleaves A Mitochondrial Complex I Protein to Initiate Caspase-Independent Cell Death. Cell 2008, 133 (4), 681-692.

32. Tournier, C.; Hess, P.; Yang, D. D.; Xu, J.; Turner, T. K.; Nimnual, A.; Bar-Sagi, D.; Jones, S. N.; Flavell, R. A.; Davis, R. J., Requirement of JNK for Stress-Induced Activation of the Cytochrome C-mediated Death Pathway. Science 2000, 288 (5467), 870-874.

33. Nagy, A., Cre Recombinase: The Universal Reagent for Genome Tailoring. Genesis 2000, 26 (2), 99-109.

34. Smith, A. J.; De Sousa, M. A.; Kwabi-Addo, B.; Heppell-Parton, A.; Impey, H.; Rabbitts, P., A Site–Directed Chromosomal Translocation Induced in Embryonic Stem Cells by Cre-Loxp Recombination. Nat. Genet. 1995, 9 (4), 376.

35. Mout, R.; Ray, M.; Tay, T.; Sasaki, K.; Yesilbag Tonga, G.; Rotello, V. M., General Strategy for Direct Cytosolic Protein Delivery via Protein-Nanoparticle Co-engineering. ACS Nano 2017, 11 (6), 6416-6421.

36. Doctor, R. B.; Dahl, R. H.; Salter, K. D.; Fouassier, L.; Chen, J.; Fitz, J. G., ATP Depletion in Rat Cholangiocytes Leads to Marked Internalization of Membrane Proteins. Hepatology 2000, 31 (5), 1045-54.

37. Lu, M.; Zak, J.; Chen, S.; Sanchez-Pulido, L.; Severson, D. T.; Endicott, J.; Ponting, C. P.; Schofield, C. J.; Lu, X., A Code for Rangdp Binding in Ankyrin Repeats Defines a Nuclear Import Pathway. Cell 2014, 157 (5), 1130-45.

38. Tang, R.; Wang, M.; Ray, M.; Jiang, Y.; Jiang, Z.; Xu, Q.; Rotello, V. M., Active Targeting of the Nucleus Using Nonpeptidic Boronate Tags. J Am Chem Soc 2017, 139 (25), 8547-8551.

39. Schavemaker, P. E.; Smiqiel, W. M.; Poolman, B., Ribosome surface properties may impose limits on the nature of the sytoplasmic proteome. Elife 2017;6:e30084

40. Thompson, D. B.; Cronican, J. J.; Liu, D. R., Engineering and Identifying Supercharged Proteins for Macromolecule Delivery into Mammalian Cells. Methods Enzymol 2012, 503, 293-319.

41. Mout, R.; Yesilbag Tonga, G.; Wang, L. S.; Ray, M.; Roy, T.; Rotello, V. M., Programmed Self-Assembly of Hierarchical Nanostructures through Protein-Nanoparticle Coengineering. ACS Nano 2017, 11 (4), 3456-3462.

42. Guo, X.; Zhang, H.; Wang, Y.; Pang, W.; Duan, X., Programmable Multi-DNA Release From Multilayered Polyelectrolytes Using Gigahertz Nano-Electromechanical Resonator. J Nanobiotechnology 2019, 17 (1), 86.

For TOC